



## Novel mercury sensor based on water soluble styrylindolium dye

Yuanyuan Li<sup>a</sup>, Fangfang Wei<sup>a</sup>, Yan Lu<sup>a,\*</sup>, Song He<sup>a</sup>, Liancheng Zhao<sup>a,b</sup>, Xianshun Zeng<sup>a,\*</sup>

<sup>a</sup>Key Laboratory of Display Materials & Photoelectric Devices, Ministry of Education, School of Materials Science & Engineering, Tianjin University of Technology, Tianjin 300384, China

<sup>b</sup>School of Materials Science and Engineering, Institute of Information Functional Materials & Devices, Harbin Institute of Technology, Harbin 150001, China

### ARTICLE INFO

#### Article history:

Received 5 February 2012

Received in revised form

14 September 2012

Accepted 17 September 2012

Available online 26 September 2012

#### Keywords:

Styrylindolium

Dye

Sensor

Fluorescence

Mercury

Intramolecular charge transfer

### ABSTRACT

A novel water soluble Hg<sup>2+</sup>-selective chemosensor using a styrylindolium dye as both colorimetric and fluorometric reporting group has been synthesized and characterized. The chemosensor exhibits a specific Hg<sup>2+</sup> selectivity to discriminate between Hg<sup>2+</sup> and chemically close ions by using a NO<sub>2</sub>S<sub>2</sub> chelating unit as the ion binding site. Due to the Hg<sup>2+</sup>-induced intramolecular charge transfer, the chemosensor shows a visible colorimetric change from red to yellow, leading to potential production of both visual and fluorometric detection of Hg<sup>2+</sup> cation both in water and in aqueous ethanol solutions.

© 2012 Elsevier Ltd. All rights reserved.

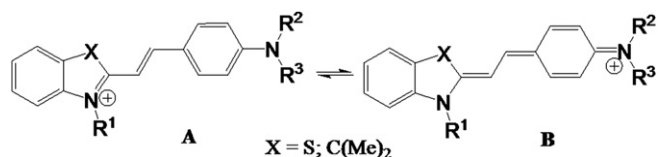
### 1. Introduction

Chromo- and fluoro-ionophores combined by an organic dye as a signaling unit and an ionophore as an ionic binding moiety within a single molecule provide a basis for the development of supra-molecular ionic devices. Many excellent ionic devices have been developed for the detection of various ions based on different signaling mechanisms, such as photo-induced electron transfer (PET) [1–5], internal charge transfer (ICT) [6–13], fluorescence resonance energy transfer (FRET) [14] and excimer [15,16]. Amongst these, the chemosensors which exhibit spectrum signal changes along with an obvious color change which provide for a rapid judgment for ion sensing, in particular, have received great attention. Herein, we aim to develop a novel visual chemosensor for Hg<sup>2+</sup>. It was known that the electronic property of an ICT sensor (e.g. UV–visible and fluorescent emission spectra) is very sensitive to the presence of ions. The feature may facilitate the kind of chemosensors to detect targeted ions by direct visual observation. Hemicyanine-based dyes have found applications in many fields, such as the study of complex biological systems as molecular probes and photosensitizers in dye-sensitized solar cells [17,18],

due to their excellent spectroscopic properties including high molar extinction coefficient ( $\epsilon \sim 10^4 \text{ M}^{-1} \text{ cm}^{-1}$ ), reasonable fluorescence quantum yield and the properties of significant spectral signal changes under external environmental stimuli. By the careful design of the ionic binding unit conjugated with the styryl dye, some hemicyanine dye-based chemosensors have also been developed by using ICT signaling mechanisms in recent years. For example, styrylbenzothiazolium dye with a crown ether as binding unit was developed for Mg<sup>2+</sup> [19], Ag<sup>+</sup>, Hg<sup>2+</sup> [20,21] and Ba<sup>2+</sup> sensing [22]. Boronic acid grafted styrylpyridinium dyes were used as cyanide fluorogenic chemosensors [23]. Merocyanine forms of spiropyran derivatives, such as the styrylindolium dye [24] and styrylbenzothiazolium dye [25], were also developed as Cu<sup>2+</sup>- and Hg<sup>2+</sup>-sensitive chemosensors, respectively.

The chemosensor based on *para*-N-substituted styrylindolium dyes has potential application as a direct visual ion sensor due to the obvious color change before and after the ion binding event. As shown in Scheme 1, due to intramolecular charge transfer between two nitrogen atoms within the chemosensor, the chemosensor exhibited the absorption and the emission in long-wavelength regions because of the equilibrium between the benzenoid form (A) and the quinoid form (B) (Scheme 1) in the absence of ions. Upon the addition of a metal ion, the fact that the lone pairs of the substituted nitrogen atom located on the *para*-position of the styryl dye participated in the ligation with the ion prevented the intramolecular charge transfer, which led to the absorption band of the

\* Corresponding author. Tel.: +86 22 6021 6748; fax: +86 22 6021 5226.  
E-mail address: xshzeng@tjut.edu.cn (X. Zeng).



**Scheme 1.** The equilibrium between the benzenoid form (A) and the quinoid form (B).

chemosensor being shifted to shorter wavelength with an associated color change.

In the present work, a novel styrylindolium dye-based, water soluble, colorimetric and fluorometric chemosensor **3** was reported as  $\text{Hg}^{2+}$ -selective chemosensor. The chemosensor **3** involves a styrylindolium dye moiety and a  $\text{NS}_2\text{O}_2$  ionophore. The  $\text{NS}_2\text{O}_2$  ionophore located on the *para*-position of the styryl dye possesses strong affinity toward the heavy metal ions similar to pendant or crown ether systems as reported in our previous work [26–28]. The chemosensor **3** shows a remarkably high selectivity to discriminate between  $\text{Hg}^{2+}$  and chemically close ions in conjunction with a visible colorimetric change from red to light yellow, leading to production of both visual and fluorometric detection of the  $\text{Hg}^{2+}$  ion due to the ligation of the electron-donor aniline nitrogen with the  $\text{Hg}^{2+}$  ion promoting a strong intramolecular charge transfer (ICT).

## 2. Experimental

### 2.1. Materials and instruments

All solvents and reagents (analytical grade and spectroscopic grade) were obtained commercially and used as received unless otherwise mentioned. pH measurements were carried out on a Mettler Toledo MP 220 pH meter. NMR spectra were recorded on a Bruker spectrometer at 400 ( $^1\text{H}$  NMR) MHz and 100 ( $^{13}\text{C}$  NMR) MHz. Chemical shifts ( $\delta$  values) were reported in ppm down field from internal  $\text{Me}_4\text{Si}$  ( $^1\text{H}$  and  $^{13}\text{C}$  NMR). EI mass spectra were recorded on a VG ZAB-HS mass spectrometer (VG, U. K.). High-resolution mass spectra (HRMS) were acquired on an Agilent 6510 Q-TOF LC/MS instrument (Agilent Technologies, Palo Alto, CA) equipped with an electrospray ionization (ESI) source. Elemental analyses were performed on a Vanio-EL elemental analyzer (Analytensystem GmbH, Germany). UV absorption spectra were recorded on a UV-3600 UV–VIS spectrophotometer (Shimadzu, Japan). Fluorescence measurements were performed using an F-4600 fluorescence spectrophotometer (Hitachi, Japan) and a quartz cell (1 cm  $\times$  1 cm). Melting points were recorded on a Boethius Block apparatus and are uncorrected.

### 2.2. General spectroscopic methods

Metal ions and the chemosensor **3** were dissolved in deionized water and ethanol to obtain 10 mM stock solutions, respectively. Before spectroscopic measurements, the solution was freshly prepared by diluting the high concentration the stock solution to the required concentration. All of the experiments were conducted at standard barometric pressure and room temperature.

### 2.3. Synthesis of 4-(*N,N*-bis-(2-hydroxyethylthiaethyl)) benzaldehyde **2**

To a 250 mL reactor, was added sodium carbonate (2.1 g, 19.8 mmol), tetrahydrofuran (50 mL), water (20 mL) and 4-(*N,N*-bis-(2-chloro-ethyl))benzaldehyde **1** (2.46 g, 10 mmol). The reaction mixture was flushed with nitrogen for 20 min, and then

2-mercaptoethanol (3.2 mL) was added in one portion. The reaction mixture was stirred for 12 h at 80 °C under nitrogen atmosphere. The reaction mixture was diluted with water (100 mL) and extracted with dichloromethane (5  $\times$  50 mL). The combined organic phase was dried over  $\text{MgSO}_4$ . After filtration, the filtrate was condensed to dryness. The residue was purified by column chromatography ( $\text{SiO}_2$ ,  $\text{CH}_2\text{Cl}_2/\text{EtOAc}$ , 4:1, v/v). The product was obtained as a viscous oil (0.924 g) in 28.0% yield; MS (EI)  $m/z$  [ $\text{M} + \text{H}$ ] $^+$ : 329.11 (Calcd); Found: 329.12; IR (KBr): 3369, 2930, 2872, 1660, 1592, 1522, 1400, 1343, 1281, 1167, 1045, 1007, 926, 815  $\text{cm}^{-1}$ .  $^1\text{H}$  NMR (400 MHz,  $\text{CDCl}_3$ , ppm)  $\delta$  9.70 (s, 1H), 7.71 (d,  $J = 8.8$  Hz, 2H), 6.68 (d,  $J = 8.8$  Hz, 2H), 3.78 (t,  $J = 6$  Hz, 4H), 3.64 (t,  $J = 7.6$  Hz, 4H), 2.78 (t,  $J = 7.2$  Hz, 8H), 2.75 (s, 2H);  $^{13}\text{C}$  NMR (100 MHz,  $\text{CDCl}_3$ , ppm): 190.41, 151.61, 132.50, 125.89, 111.13, 61.41, 51.54, 35.44, 29.20; Anal. Calcd for  $\text{C}_{15}\text{H}_{23}\text{NO}_3\text{S}_2 \cdot 0.75\text{H}_2\text{O}$ : C 52.53%, H 7.20%, N 4.08%; Found: C 52.60%, H 7.37%, N 3.93%.

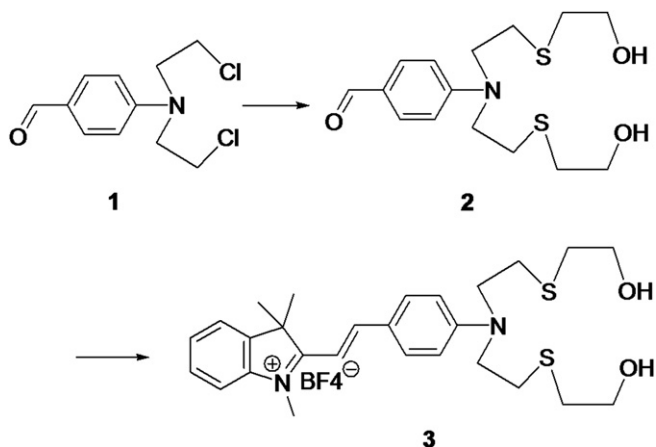
### 2.4. Preparation of the chemosensor tetrafluoroborate of 2-[2-[4-*N,N'*-bis(2-hydroxyethylthio-ethyl)aminophenyl]ethenyl]-1,3,3'-trimethylindoline **3**

To a 50 mL round-bottomed flask, was charged *N*-methyl-2,3,3'-trimethylindolium iodide (0.51 g, 1.55 mmol), compound **2** (0.462 g, 1.54 mmol) and ethanol (8 mL). The reaction suspension was flushed with nitrogen for 20 min, and then stirred for 14 h at 95 °C. After cooling, the reaction mixture was condensed to dryness. The residue was purified by column chromatography ( $\text{SiO}_2$ ,  $\text{CH}_2\text{Cl}_2/\text{EtOH}$ , 10:1, v/v). The product was obtained as red powder (0.824 g) in 87.7% yield. The product was dissolved in ethanol (20 mL) and dichloromethane (20 mL), and then  $\text{NaBF}_4$  (1 g) was added. The reaction mixture was stirred at 50 °C for 2.5 h in dark. The solid inorganic salts were filtered out. The filtrate was condensed to dryness. The residue was dried under vacuum to get a red powder (0.883 g) in 99% yield. HRMS:  $m/z$  [ $\text{M} + \text{H}$ ] $^+$  485.2291 (Calcd); Found: 485.2295; IR (KBr), 3354, 3025, 2918, 2861, 1571, 1521, 1466, 1402, 1283, 1173, 1109, 1046, 980, 931, 786, 752, 717  $\text{cm}^{-1}$ .  $^1\text{H}$  NMR (400 MHz,  $\text{D}_2\text{O}$ , ppm): 8.15 (d,  $J = 1.2$  Hz, 2H), 8.06 (s, 1H), 7.49–7.32 (m, 5H), 6.91 (d,  $J = 8.8$  Hz, 2H), 4.16 (s, 3H), 3.86 (t,  $J = 5.8$  Hz, 4H), 3.75 (t,  $J = 7.8$  Hz, 4H), 2.91–2.78 (m, 8H), 1.79 (s, 6H);  $^{13}\text{C}$  NMR (100 MHz, DMSO, ppm): 179.74, 153.57, 151.99, 142.35, 141.71, 133.81, 128.45, 127.50, 122.47, 122.30, 113.44, 112.00, 105.48, 60.83, 50.47, 34.00, 32.92, 28.67, 25.90. Anal. Calcd for  $\text{C}_{27}\text{H}_{37}\text{BF}_4\text{N}_2\text{O}_2\text{S}_2$ : C 56.64%, H 6.51%, N 4.89%; Found: C 56.88%, H 6.43%, N 4.70%.

## 3. Results and discussion

### 3.1. The molecular design and preparation of the chemosensor **3**

We present here a novel, highly sensitive fluorescent chemosensor based on a styrylindolium dye (Scheme 2), which displayed high  $\text{Hg}^{2+}$  selectivity both in water and ethanol/water mixture by using the internal charge-transfer (ICT) mechanism. The chemosensor **3** composed of an electron-donor aniline moiety and an electron acceptor that in this case is a styrylindolium dye where the electron-donor nitrogen atom, sulfur atoms and the hydroxyl oxygen atoms provide the mercury-coordinating elements [29,30]. The chemosensor **3** was synthesized from **1** through two steps. As shown in Scheme 1, aldehyde **2** was obtained by the reaction of **1** with sodium salt of 2-mercaptoethanol prepared in the presence of  $\text{Na}_2\text{CO}_3$  as a base. Then, **3** was readily prepared in 99% yield by the condensation of *N*-methyl-2,3,3'-trimethylindolium iodide with **2** in ethanol under refluxed. The anion exchange was carried out by refluxing the ethanol solutions **3** with excess  $\text{NaBF}_4$ . The structure of **3** was confirmed by MS, NMR and elemental analyses.



Scheme 2. The preparation of chemosensor **3**.

### 3.2. UV–Vis evaluation of metal binding interaction

The chemosensor **3** is soluble in H<sub>2</sub>O or in aqueous ethanol. Therefore, the sensing behavior was carried out both in water and in ethanol/water systems for comparison the differences of the binding ability of **3** toward metal ions in different solvent systems, which may provide more valuable information for new receptor design. Fig. 1 displays the absorption spectra of the chemosensor **3** in the presence and absence of a variety of environmentally and biologically relevant metal ions. The UV/Vis spectra of **3** both in H<sub>2</sub>O and in aqueous ethanol show the characteristic intense charge-transfer band occurring in the long-wavelength region between 425 and 600 nm, which centered at 540 nm in water ( $\epsilon = 8.7 \times 10^4 \text{ M}^{-1} \text{ cm}^{-1}$ ) and 525 nm in EtOH/H<sub>2</sub>O (1:1, v/v) ( $\epsilon = 7.8 \times 10^4 \text{ M}^{-1} \text{ cm}^{-1}$ ) (Fig. 1a and 1b). As shown in Fig. 1a and 1b, upon addition 50 equivalents of Hg<sup>2+</sup>, the absorbance band over 500 nm vanished drastically, while the one around 400 nm increased significantly. There was over a 30-fold decrease in absorbance at ca. 530 nm and with a large enhancement factor (over 15-fold) of absorbance at ca. 400 nm upon the addition of 50 equivalents of Hg<sup>2+</sup>. This interesting feature revealed that **3** can serve as selective visual chemosensor for Hg<sup>2+</sup> (Fig. S1). Upon addition the other metal ions such as K<sup>+</sup>, Na<sup>+</sup>, NH<sub>4</sub><sup>+</sup>, Al<sup>3+</sup>, Co<sup>2+</sup>, Fe<sup>3+</sup>, Pb<sup>2+</sup>, Cu<sup>2+</sup>, Zn<sup>2+</sup>, Cd<sup>2+</sup>, Ni<sup>2+</sup>, Ca<sup>2+</sup>, Mg<sup>2+</sup>, no significant changes in the UV spectra were observed both in H<sub>2</sub>O and in aqueous ethanol (Fig. 1), except for Ag<sup>+</sup> which displays a slight decrease of the absorbance at 540 nm. The large changes in the spectrum by the addition of Hg<sup>2+</sup> implied that the electron-donor aniline nitrogen participated the ligation with the Hg<sup>2+</sup> ion which promoted intramolecular charge-transfer (ICT) process occurred as shown in Scheme 3. The unique absorption change by the addition of Hg<sup>2+</sup> implied that the chemosensor **3** was efficiently binding with Hg<sup>2+</sup> selectively. Normally, free Hg<sup>2+</sup> only exists in strong acidic media (pH < 2), while at pH > 2, Hg<sup>2+</sup> usually exists in the form of Hg(OH)<sup>+</sup>[31]. Therefore, the high selectivity can be rationalized that the Hg(OH)<sup>+</sup> was not only selectively entrapped by the NS<sub>2</sub>O<sub>2</sub> chelating unit but also further stabilized by the formation of intramolecular O–H...O hydrogen bonds as shown in Scheme 3.

To obtain further insight into the binding of Hg<sup>2+</sup> with **3**, the absorption spectra of **3** upon titration with Hg<sup>2+</sup> were recorded in H<sub>2</sub>O (Fig. 2a). For comparison the binding ability of **3** with Hg<sup>2+</sup>, the absorption spectra of **3** upon titration with Hg<sup>2+</sup> were also recorded in aqueous ethanol (ethanol/water, 1:1, v/v) solutions (Fig. 2b). With the addition of Hg<sup>2+</sup>, the absorbance at 540 nm in aqueous ethanol and 525 nm in water decreased sharply, while the band at

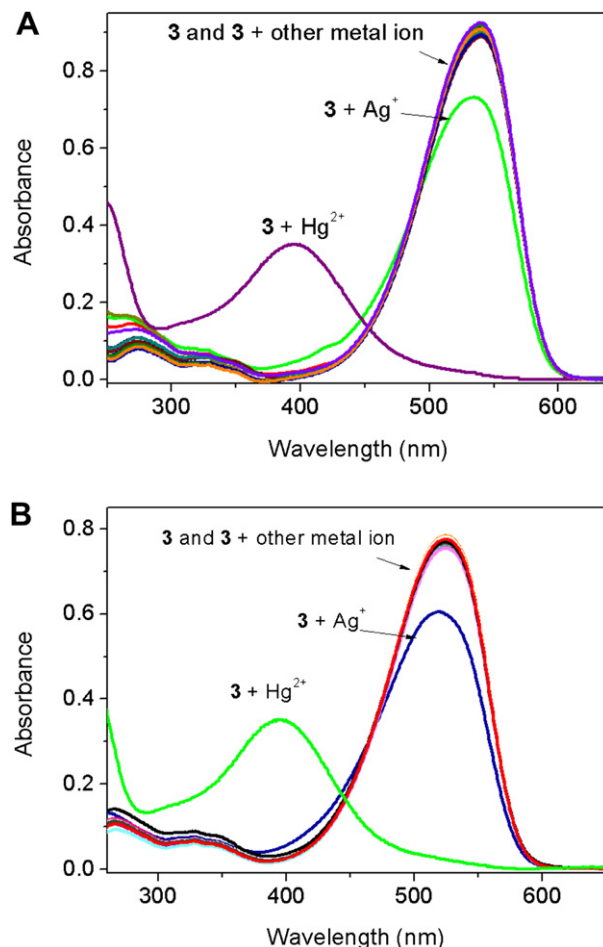
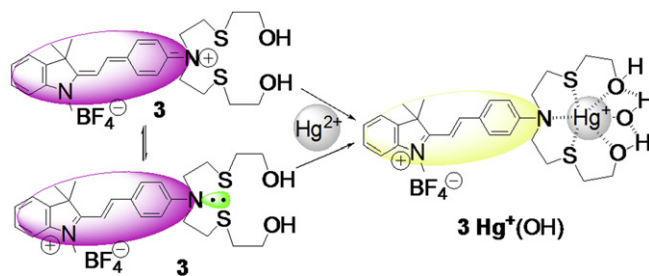
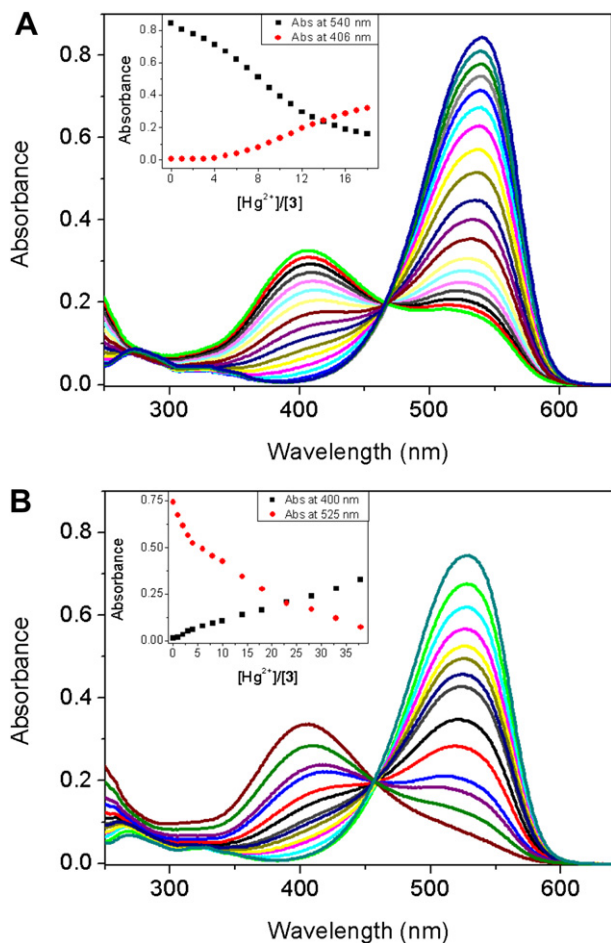


Fig. 1. UV–vis responses of chemosensor **3** (10  $\mu\text{M}$ ) upon the addition of the nitrate salts (50.0 equiv) of Na<sup>+</sup>, K<sup>+</sup>, NH<sub>4</sub><sup>+</sup>, Mg<sup>2+</sup>, Ca<sup>2+</sup>, Pb<sup>2+</sup>, Hg<sup>2+</sup>, Co<sup>2+</sup>, Cd<sup>2+</sup>, Zn<sup>2+</sup>, Ni<sup>2+</sup>, Cu<sup>2+</sup>, Cr<sup>3+</sup>, Fe<sup>3+</sup> and Ag<sup>+</sup> (a) in ethanol/H<sub>2</sub>O (1:1, v/v) and (b) in H<sub>2</sub>O.

406 nm in aqueous ethanol and 400 nm in water increased significantly. Meanwhile, the isosbestic points at 466 nm in EtOH/H<sub>2</sub>O (1:1, v/v) and 455 nm in H<sub>2</sub>O were observed indicated the formation of a new complex between **3** and Hg<sup>2+</sup>. The changes of the absorbance at ca. 530 nm and at ca. 400 nm with the increase of [Hg<sup>2+</sup>] were shown in the inset of Fig. 2a and 2b. It is important to note that a 1:1 stoichiometry for the **3**•Hg<sup>2+</sup> complex was confirmed by Job's plot analysis [32], where the decrease of the absorbance at 525 nm was plotted against mole fractions of **3** under the conditions of a constant total concentration of [**3**] + [Hg<sup>2+</sup>]. As such, the concentration of the **3**•Hg<sup>2+</sup> complex approached a maximum when the molar fraction of [**3**]/[Hg<sup>2+</sup>] was about 1



Scheme 3. The equilibrium between the benzenoid form and the quinoid form of **3** and the coordination model of **3** and Hg<sup>2+</sup>.



**Fig. 2.** Absorbance spectra of **3** (10  $\mu\text{M}$ ) (a) in  $\text{H}_2\text{O}$  and (b) in  $\text{EtOH}/\text{H}_2\text{O}$  (1:1, v/v) in the presence of different amounts of  $\text{Hg}^{2+}$ . (a)  $[\text{Hg}^{2+}]/[\mathbf{3}]$ : 0, 1, 2, 3, 4, 5, 6, 7, 8, 9, 10, 11, 12, 13, 14, 15, 16, 17, 18 in  $\text{EtOH}/\text{H}_2\text{O}$  (1:1, v/v), Inset: the changes of the absorbance at 540 nm and absorbance at 406 nm as a function of  $\text{Hg}^{2+}$  concentration. (b)  $[\text{Hg}^{2+}]/[\mathbf{3}]$ : 0, 1, 2, 3, 4, 6, 8, 10, 14, 18, 23, 28, 33, 38 in  $\text{H}_2\text{O}$ , Inset: the changes of the absorbance at 525 nm and absorbance at 400 nm as a function of  $\text{Hg}^{2+}$  concentration.

(Fig. S2). From the changes in  $\text{Hg}^{2+}$ -dependent absorption intensity, the detection limit was estimated to be  $1.5 \times 10^{-7}$  M in water (Fig. S3).

### 3.3. Metal ion binding studies by fluorescence titration

Subsequently, the nitrate salts of  $\text{K}^+$ ,  $\text{Na}^+$ ,  $\text{NH}_4^+$ ,  $\text{Al}^{3+}$ ,  $\text{Co}^{2+}$ ,  $\text{Fe}^{3+}$ ,  $\text{Pb}^{2+}$ ,  $\text{Ag}^+$ ,  $\text{Cu}^{2+}$ ,  $\text{Zn}^{2+}$ ,  $\text{Cd}^{2+}$ ,  $\text{Ni}^{2+}$ ,  $\text{Ca}^{2+}$ ,  $\text{Mg}^{2+}$  and  $\text{Hg}^{2+}$  ions were used to evaluate the metal ion binding property and selectivity of the chemosensor **3** (10  $\mu\text{M}$ ) by fluorescence spectra in  $\text{H}_2\text{O}$ . As shown in Fig. 3, an emission band centered at 590 nm of the free chemosensor **3** (10  $\mu\text{M}$ ) was observed. Upon the addition of 10 equivalents of  $\text{Na}^+$ ,  $\text{K}^+$ ,  $\text{NH}_4^+$ ,  $\text{Mg}^{2+}$ ,  $\text{Ca}^{2+}$ ,  $\text{Pb}^{2+}$ ,  $\text{Co}^{2+}$ ,  $\text{Cd}^{2+}$ ,  $\text{Zn}^{2+}$ ,  $\text{Ni}^{2+}$ ,  $\text{Cr}^{3+}$ ,  $\text{Fe}^{3+}$ , and  $\text{Al}^{3+}$ , no obvious effect on the fluorescence emissions were observed, whereas  $\text{Ag}^+$  responded with weak decrease in the fluorescent intensity. In contrast, the addition of  $\text{Hg}^{2+}$  resulted in a significant diminution of the emission intensity at 590 nm. The fact that **3** showed a strong fluorescence diminution only with  $\text{Hg}^{2+}$  among the various metal ions examined indicated that **3** displayed a high  $\text{Hg}^{2+}$  selectivity. The fluorescence spectra were obtained by excitation of the hemicyanine fluorophore at 520 nm.

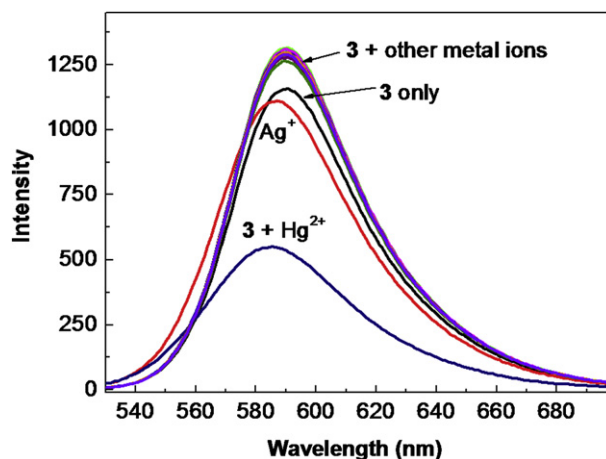


**Fig. 3.** Fluorescence spectra of **3** (10  $\mu\text{M}$ ) upon the addition of the nitrate salts (10 equiv.) of  $\text{Na}^+$ ,  $\text{K}^+$ ,  $\text{NH}_4^+$ ,  $\text{Ag}^+$ ,  $\text{Mg}^{2+}$ ,  $\text{Ca}^{2+}$ ,  $\text{Pb}^{2+}$ ,  $\text{Hg}^{2+}$ ,  $\text{Co}^{2+}$ ,  $\text{Cd}^{2+}$ ,  $\text{Zn}^{2+}$ ,  $\text{Ni}^{2+}$ ,  $\text{Cu}^{2+}$ ,  $\text{Cr}^{3+}$ ,  $\text{Fe}^{3+}$ , and  $\text{Al}^{3+}$  in  $\text{H}_2\text{O}$  ( $\lambda_{\text{ex}} = 520$  nm).

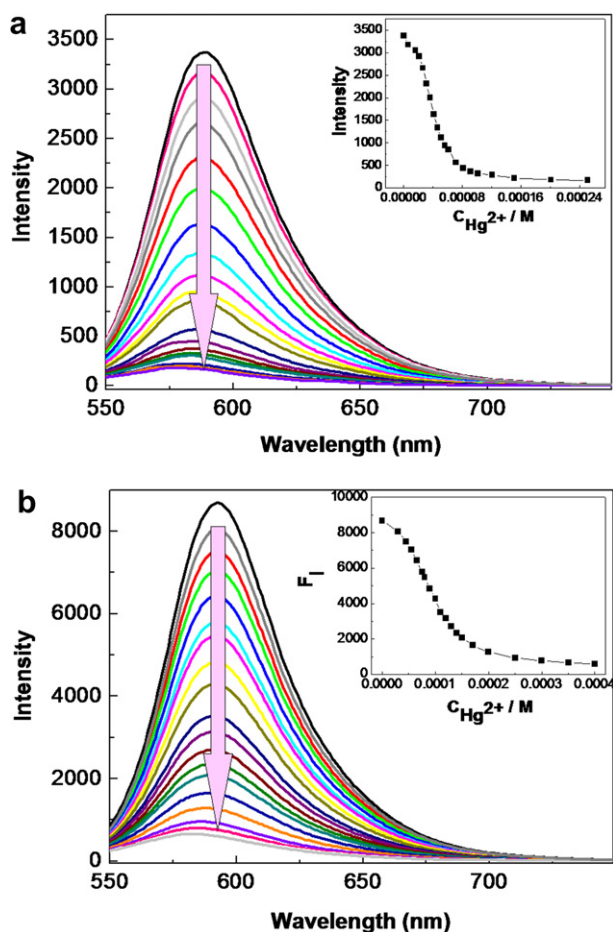


**Fig. 4.** Fluorescent titration spectra. (a) **3** (10  $\mu\text{M}$ ) in the presence of different concentrations of  $\text{Hg}^{2+}$  in water,  $[\text{Hg}^{2+}] = 0, 6, 16, 21, 26, 31, 36, 41, 46, 51, 56, 61, 71, 81, 91, 101, 121, 151, 201, 251$  equivalents. Inset: Fluorescent intensity  $F_i$  as a function of  $\text{Hg}^{2+}$  concentration.  $\lambda_{\text{ex}} = 530$  nm. (b) **3** (10  $\mu\text{M}$ ) in the presence of different concentrations of  $\text{Hg}^{2+}$  in ethanol/water (1:1, v/v),  $[\text{Hg}^{2+}] = 0, 30, 45, 55, 65, 75, 90, 100, 110, 120, 130, 140, 150, 170, 200, 250, 300, 350, 400$  equivalents. Inset: Fluorescent intensity ( $F_i$ ) as a function of  $\text{Hg}^{2+}$  concentration.  $\lambda_{\text{ex}} = 530$  nm.

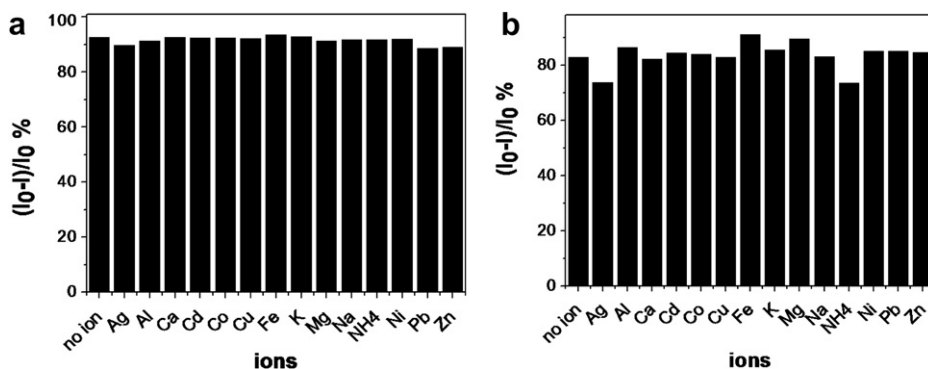


Fig. 5.  $(I_0 - I)/I_0$  ratio of fluorescence intensity of **3** (10  $\mu$ M) upon the addition of 50 equivalents  $\text{Hg}^{2+}$  in the presence of 50 equivalents background metal ions. (a) In  $\text{H}_2\text{O}$  and (b) in  $\text{EtOH}/\text{H}_2\text{O}$  (1:1, v/v) solution.

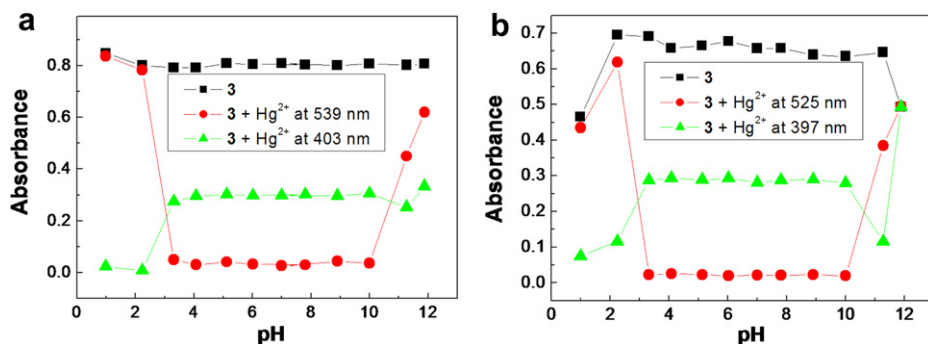


Fig. 6. pH profiles of the absorption intensities of **3** (10  $\mu$ M) in the absence and presence of  $\text{Hg}^{2+}$  (10 eqv.) in  $\text{EtOH}/\text{H}_2\text{O}$  (1:1, v/v) (a) and in  $\text{H}_2\text{O}$  (b).

To achieve a binding constant ( $K$ ) via fluorescence titration, the titrations were conducted in  $\text{H}_2\text{O}$  solutions. Fig. 4a shows the gradual change of the fluorescence spectra of **3** upon addition of  $\text{Hg}^{2+}$ , clear “on-off” fluorescence changes of **3** to  $\text{Hg}^{2+}$  were observed. When  $\text{Hg}^{2+}$  was added to the solution, a significant decrease of the fluorescence intensity at 590 nm and with a blue shift to 576 nm was observed. The quenching is found to follow a Benesi–Hildebrand equation. A linear dependence of the ratio of fluorescent intensity  $[\text{3}][\text{Hg}^{2+}]/(F_0 - F_i)$  at 590 nm as a function of  $\text{Hg}^{2+}$  concentration assumed a 1:1 stoichiometry for the  $\text{3}\cdot\text{Hg}^{2+}$  complex. The binding constant derived from the fluorogenic titrations was found to be  $3.46 \times 10^4 \text{ M}^{-1}$  ( $R = 0.992$ ) in water. For comparison, the fluorometric titrations of **3** with  $\text{Hg}^{2+}$  were also recorded in aqueous ethanol (ethanol/water, 1:1, v/v) solutions (Fig. 4b). The binding constant was found to be  $1.17 \times 10^4 \text{ M}^{-1}$  ( $R = 0.994$ ) in aqueous ethanol, indicating that the binding ability of **3** in aqueous ethanol is weaker than that in water. From the changes in  $\text{Hg}^{2+}$ -dependent fluorescence intensity, the detection limit was estimated to be  $1.0 \times 10^{-7} \text{ M}$  (Fig. S4) [33], indicating that the limit of detection of **3** to  $\text{Hg}^{2+}$  met the discharge limits for industrial waste water according to the China SA standard [34].

#### 3.4. Selective binding of $\text{Hg}^{2+}$

To explore further the utility of the chemosensor **3** as an ion-selective fluorescent chemosensor for  $\text{Hg}^{2+}$ , ion interference experiments were carried out both in  $\text{H}_2\text{O}$  and in aqueous ethanol (ethanol/water, 1:1, v/v) solvent systems for evaluation of the sensing ability of **3** toward  $\text{Hg}^{2+}$  in the presence of 50 equivalents of a series of background metal ions. The results are shown in Fig. 5. No interference was observed in  $\text{H}_2\text{O}$  in the presence of 50 equivalents of a series of metal ions (Fig. 5a). It showed the same tendency in aqueous ethanol (Fig. 5b). In both cases, almost no

color change is observed in the presence of metal ions other than  $\text{Hg}^{2+}$ . When 50 equivalents of  $\text{Hg}^{2+}$  are added to these solutions, the red color disappears immediately and the spectra are almost identical to that obtained in the presence of  $\text{Hg}^{2+}$  alone. The results demonstrated that the chemosensor **3** is able to discriminate between  $\text{Hg}^{2+}$  and chemically close ions, especially  $\text{Ag}^+$  which is common interfering ion in many cases. Obviously, the remarkable sensitivity for fluorescent detection of  $\text{Hg}^{2+}$  can be available using the chemosensor **3** even in the presence of coexisting metal ions.

#### 3.5. pH profiles of chemosensor **3**

For practical applicability, the proper pH condition of the chemosensor **3** was evaluated in the presence and absence of  $\text{Hg}^{2+}$  by absorption spectra. The absorption intensities at different pH values of the free and  $\text{Hg}^{2+}$ -bound forms of **3** in  $\text{EtOH}/\text{H}_2\text{O}$  (1:1, v/v) and in water are shown in Fig. 6. As can be seen from Fig. 6, absorption intensities are essentially insensitive to pH in the pH range of 3–10 in both cases. Thus, the chemosensor **3** can be used for  $\text{Hg}^{2+}$  detection in a wide pH range, which is convenient for the practical application.

## 4. Conclusion

In conclusion, a styrylindolium dye with a  $\text{NS}_2\text{O}_2$  ionophore on the *para*-position of the styryl moiety has been successfully designed and synthesized as a  $\text{Hg}^{2+}$ -selective chemosensor by taking advantage of the ICT mechanism. Results revealed that the chemosensor **3** could be used as an efficient  $\text{Hg}^{2+}$ -selective fluorescent and chromogenic chemosensor both in aqueous ethanol solution and in water. The detection limit for  $\text{Hg}^{2+}$  was determined as  $1.0 \times 10^{-7} \text{ M}$ . The chemosensor shows a remarkably high selectivity to discriminate between  $\text{Hg}^{2+}$  and chemically close ions in

conjunction with a visible colorimetric change from red to light yellow, leading to production of both visual and fluorometric detection of the  $\text{Hg}^{2+}$  ion due to the ligation of the electron-donor aniline nitrogen with the  $\text{Hg}^{2+}$  ion promoting a strong intramolecular charge transfer (ICT).

### Acknowledgments

This work was sponsored by the NNSFC (21272172, 20972111, 21074093, 21004044), NCET-09-0894, SRF for ROCS, SEM, the NSFT (12JCZDJ21000) and the State Key Lab. Elemental-Organic Chemistry at Nankai University (No. 1103).

### Appendix A. Supplementary data

Supplementary data related to this article can be found at <http://dx.doi.org/10.1016/j.dyepig.2012.09.010>

### References

- Nolan EM, Lippard SJ. Tools and tactics for the optical detection of mercuric ion. *Chemical Reviews* 2008;108:3443–80.
- Guo X, Qian X, Jia L. A highly selective and sensitive fluorescent chemosensor for  $\text{Hg}^{2+}$  in neutral buffer aqueous solution. *Journal of the American Chemical Society* 2004;126:2272–3.
- Prodi L, Bargossi C, Montalti M, Zaccaroni N, Su N, Bradshaw JS, Izatt RM, Savage PB. An effective fluorescent chemosensor for mercury ions. *Journal of the American Chemical Society* 2000;122:6769–70.
- Lu Y, Huang S, Liu Y, He S, Zhao L, Zeng X. Highly selective and sensitive fluorescent turn-on chemosensor for  $\text{Al}^{3+}$  based on a novel photoinduced electron transfer approach. *Organic Letters* 2011;13:5274–7.
- Huang S, He S, Lu Y, Wei F, Zeng X, Zhao L. Highly sensitive and selective fluorescent chemosensor for  $\text{Ag}^+$  based on a coumarin- $\text{Se}_2\text{N}$  chelating conjugate. *Chemical Communications* 2011;47:2408–10.
- Ros-Lis JV, Martínez-Mañez R, Rurack K, Sancenón F, Soto J, Spieles M. Highly selective chromogenic signaling of  $\text{Hg}^{2+}$  in aqueous media at nanomolar levels employing a squaraine-based reporter. *Inorganic Chemistry* 2004;43:5183–5.
- Wang J, Qian X. Two regioisomeric and exclusively selective  $\text{Hg}(\text{II})$  sensor molecules composed of a naphthalimide fluorophore and an *o*-phenylenediamine derived triamide receptor. *Chemical Communications* 2006:109–11.
- Brümmer O, La Clair JJ, Janda KD. A colorimetric ligand for mercuric ion. *Organic Letters* 1999;1:415–8.
- Hu R, Feng J, Hu D, Wang S, Li S, Li Y, Yang G. A rapid aqueous fluoride ion sensor with dual output modes. *Angewandte Chemie International Edition* 2010;49:4915–8.
- Rurack K, Kollmannsberger M, Resch-Genger U, Daub JA. Selective and sensitive fluoroionophore for  $\text{Hg}(\text{II})$ ,  $\text{Ag}(\text{I})$ , and  $\text{Cu}(\text{II})$  with virtually decoupled fluorophore and receptor units. *Journal of the American Chemical Society* 2000;122:968–9.
- Sakamoto H, Ishikawa J, Nakao S, Wada H. Excellent mercury(II) ion selective fluoroionophore based on a 3,6,12,15-tetrathia-9-azaheptadecane derivative bearing a nitrobenzoxadiazolyl moiety. *Chemical Communications* 2000: 2395–6.
- Martínez-Mañez R, Radeglia R, Rurack K, Soto J. Coupling selectivity with sensitivity in an integrated chemosensor framework: design of a  $\text{Hg}^{2+}$ -responsive probe, operating above 500 nm. *Journal of the American Chemical Society* 2003;125:3418–9.
- Li Y, He S, Lu Y, Zeng X. Novel hemicyanine dye as colorimetric and fluorometric dual-modal chemosensor for mercury in water. *Organic & Biomolecular Chemistry* 2011;9:2606–9.
- Zhang X, Xiao Y, Qian X. A ratiometric fluorescent probe based on FRET for imaging  $\text{Hg}^{2+}$  ions in living cells. *Angewandte Chemie International Edition* 2008;47:8025–9.
- Lekha PK, Prasad E. Aggregation-controlled excimer emission from anthracene-containing polyamidoamine dendrimers. *Chemistry – A European Journal* 2010;16:3699–706.
- Xu Z, Singh NJ, Lim J, Pan J, Kim HN, Park S, Kim KS, Yoon J. Unique sandwich stacking of pyrene-adenine-pyrene for selective and ratiometric fluorescent sensing of ATP at physiological pH. *Journal of the American Chemical Society* 2009;131:15528–33.
- Mishra A, Behera RK, Behera PK, Mishra BK, Behera GB. Cyanines during the 1990s: a review. *Chemical Reviews* 2000;100:1973–2011.
- Würthner F, Kaiser TE, Saha-Möller CR. J-Aggregates: from serendipitous discovery to supramolecular engineering of functional dye materials. *Angewandte Chemie International Edition* 2011;50:3376–410.
- Barzykin AV, Fox MA, Ushakov EN, Stanislavsky OB, Gromov SP, Fedorova OA, Alfimov MV. Dependence of metal ion complexation and intermolecular aggregation on photoinduced geometric isomerism in a crown ether styryl dye. *Journal of the American Chemical Society* 1992;114:6381–5.
- Alfimov MV, Fedorov YV, Fedorova OA, Gromov SS, Hester RE, Lednev IK, Moore JN, Oleshko VP, Vedernikov AI. Synthesis and spectroscopic studies of novel photochromic benzodithiacrown ethers and their complexes. *Journal of the Chemical Society, Perkin Transactions* 1996;2:1441–7.
- Tulyakova EV, Fedorova OA, Fedorov YV, Jonusauskas G, Anisimov AV. Spectroscopic study of mono- and bis(styryl) dyes of the pyridinium series containing azathiocrown ether residue. *Journal of Physical Organic Chemistry* 2008;21:372–80.
- Alfimov MV, Churakov AV, Fedorov YV, Fedorova OA, Gromov SP, Hester RE, Howard JAK, Kuz'mina LG, Lednev IK, Moore JN. Structure and ion-complexing properties of an aza-15-crown-5 ether dye: synthesis, crystallography, NMR spectroscopy, spectrophotometry and potentiometry. *Journal of the Chemical Society, Perkin Transactions* 1997;2:2249–56.
- Badugu R, Lakowicz JR, Geddes CD. Enhanced fluorescence cyanide detection at physiologically lethal levels: reduced ICT-based signal transduction. *Journal of the American Chemical Society* 2005;127:3635–41.
- Tatay S, Gaviña P, Coronado E, Palomares E. Optical mercury sensing using a benzothiazolium hemicyanine dye. *Organic Letters* 2006;8:3857–60.
- Guo ZQ, Chen WQ, Duan XM. Highly selective visual detection of  $\text{Cu}(\text{II})$  utilizing intramolecular hydrogen bond-stabilized merocyanine in aqueous buffer solution. *Organic Letters* 2010;12:2202–5.
- Zeng X, Leng X, Chen L, Sun H, Xu F, Li Q, He X, Zhang ZZ. Novel bis(phenylseleno-alkoxy)calix[4]arene molecular tweezer receptors as sensors for ion-selective electrodes. *Journal of the Chemical Society, Perkin Transactions* 2002;2:796–801.
- Zeng X, Han X, Chen L, Li Q, Xu F, He X, Zhang ZZ. The first synthesis of a calix [4]([diseleno])crown ether as a sensor for ion-selective electrodes. *Tetrahedron Letters* 2002;43:131–4.
- Zeng X, Sun H, Chen L, Leng X, Xu F, Li Q, He X, Zhang W, Zhang ZZ. Synthesis of a tweezer-like bis(arylthioalkoxy)calix[4]arene as a cation sensor for ion-selective electrodes: an investigation of the influence of neighboring halogen atoms on cation selectivity. *Organic & Biomolecular Chemistry* 2003; 1:1073–9.
- Zeng X, Weng L, Chen L, Leng X, Ju H, He X, Zhang ZZ. The synthesis of some pyridyl functionalized calix[4]arenes as the sensor molecule for silver ion-selective electrodes. *Journal of the Chemical Society, Perkin Transactions* 2001;2:545–9.
- Qin D, Zeng X, Xu F, Li Q, Zhang ZZ. Synthesis, structure and ion extraction properties of novel mono-oxa-diselkylene-1, $\omega$ -dioxy substituted calix[4]arene derivatives. *Chinese Journal of Chemistry* 2006;24:674–80.
- a) Hietanen S, Sillén LG. Studies on the hydrolysis of metal ions II. The hydrolysis of the mercury(II) ion  $\text{Hg}^{2+}$ . *Acta Chemica Scandinavica* 1952;6: 747–58; b) Zeng X, Weng L, Chen L, Xu F, Li Q, Leng X, He X, Zhang Z. The syntheses and  $\text{Ag}^+$ -selective electrode properties of benzothiazolylthioalkoxy functionalized calix[4]arenes: an investigation of the structure-selectivity relationship in the ionophore-based ISEs. *Tetrahedron* 2002;58:2647–58.
- Connors KA. Binding constants. New York: Wiley; 1987.
- Che Y, Yang X, Zang L. Ultrasensitive fluorescent sensing of  $\text{Hg}^{2+}$  through metal coordination induced molecular aggregation. *Chemical Communications* 2008:1413–5.
- Standardization Administration (SA) of the People's Republic of China, Integrated Wastewater Discharge Standard, GB 8978, 1996.